Design of guided-wave grating-assisted tunable filters for telecommunications systems

Vittorio M. N. Passaro

Optoelectronics Laboratory, Dipartimento di Elettrotecnica ed Elettronica
Politecnico di Bari, Via Edoardo Orabona 4 – 70125 Bari, Italy
passaro@poliba.it

Abstract: In this paper, a number of critical aspects in the design and performance of guided-wave grating-assisted tunable filters for dense telecommunications systems are investigated by using a rigorous numerical approach. It is shown how highly narrow filters, with the potential to be tunable over a large number of channels (> 50), can be accurately designed by using well-selected apodization windows.

OCIS Codes: (050.2770) Gratings; (130.2790) Guided waves; (230.3120) Integrated optics devices.

References and links

1. C.R. Doerr, M. Zirngibl, C.H. Joyner, L.W. Stulz, and H.M. Presby, "Polarization Diversity Waveguide Grating Receiver with Integrated Optical Preamplifiers," IEEE Photon. Tech. Lett. **9**, 85-87 (1997).
2. J. Sapriel, D. Charissoux, V. Voloshinov and V. Molchanov, "Tunable Acoustooptic Filters and Equalizers for WDM Applications," J. Lightwave Technol. **20**, 864-871 (2002).
3. H. Sakata, "Sidelobe suppression in grating-assisted wavelength-selective couplers," Opt. Lett. **17**, 463-465 (1992).
4. R. C. Alferness and P.S. Cross, "Filter characteristics of codirectionally coupled waveguides with weighted coupling," IEEE J. Quantum Electron. **QE-14**, 843-847 (1978).
5. B. E. Little, C. Wu, and W.-P. Huang, "Synthesis of codirectional couplers with ultralow sidelobes and minimum bandwidth," Opt. Lett. **20**, 1259-1261 (1995).
6. W. P. Huang, J. Hong, and Z. M. Mao, "Improved coupled-mode formulation based on composite modes for parallel grating-assisted co-directional couplers," IEEE J. Quantum Electron. **29**, 2805-2812 (1993).
7. V.M.N. Passaro and M.N. Armenise, "Analysis of Radiation Loss in Grating-Assisted Codirectional Couplers," IEEE J. Quantum Electron. **31**, 1691-1697 (1995).
8. N.-H. Sun, J.K. Butler, G.A. Evans, L. Pang, and P. Congdon, "Analysis of Grating-Assisted Directional Couplers Using the Floquet-Bloch Theory," J. Lightwave Technol. **15**, 2301-2314 (1997).
9. V.M.N. Passaro, "Optimal Design of Grating-Assisted Directional Couplers," J. Lightwave Technol. **18**, 973-984 (2000).
10. Yu-H. Jan, G.A. Fish, L.A. Coldren, S. P. DenBaars, "Widely tunable integrated filter/receiver with apodized grating-assisted codirectional coupler," Proc. SPIE **3290**, 258-261 (1997).
11. Yu-H. Jan, G.A. Fish, L.A. Coldren, S. P. DenBaars, "Demonstration of InP-InGaAsP Vertical Grating-Assisted Codirectional Coupler Filters and Receivers with Tapered Coupling Coefficient Distributions," IEEE Photon. Tech. Lett. **9**, 994-996 (1997).
12. BeamProp by Rsoft Inc., 1999.

1. Introduction

Wavelength-selective tunable filters are fundamental devices for dense wavelength-division-multiplexing (DWDM) telecommunications systems, because of their properties to select appropriate wavelengths with very narrow bandwidth among a large number of desired channels from an incoming data stream. Together with the selectivity, the tunability is the other important property of such devices. Different architectures of guided-wave WDM filters have been presented in the literature based on arrayed waveguide grating (AWG) structures [1], showing good channel separation and side-lobe suppression ratio (SSR), but their

#1787 - $15.00 US Received October 28, 2002; Revised November 11, 2002

applicability is limited because they are not tunable. Very good performance have been also obtained by the guided-wave architectures based on acousto-optic collinear interaction [2], which have very good channel separation and SSR.

In recent years, much research effort has been devoted to improve the performance of grating-assisted directional coupler (GADC) filters [3-4]. These structures can be highly wavelength-selective and tunable over a large range, and their architectures are fully compatible with integrated semiconductor heterostructure lasers (DBR, DFB), allowing a complete monolithic integration. The working principle is based on the directional coupling of the mode travelling along the upper slab to the lower one due to the presence of the grating (first stage of the filter, as in Fig.1), and then on the second coupling from the lower to the upper slab, due to another grating (second stage). Each filter is so formed by two GADCs, each one with different geometric parameters (grating period, length, duty cycle, and so on). The wavelength selectivity can be achieved by apodizing in both stages the coupling strength between the two slabs according to a selected function along the GADC length (apodization window). The properties of the filter in terms of bandwidth and SSR are strictly related to the choice of these windows. In fact, the spectral response of each GADC is given by the FFT of the coupling coefficient distribution along the same GADC [5]. Therefore, a filter with two GADCs, each having uniform distribution of coupling coefficient (rectangular profile), is characterized by an amplitude spectral response following a $\sin c^2(f)$-like function (two cascade rectangular windows), i.e. a SSR less than –14 dB. In order to improve the selectivity of such devices, appropriate apodization windows of the coupling strength must be achieved, using functions having very narrow spectral responses and very high SSRs.

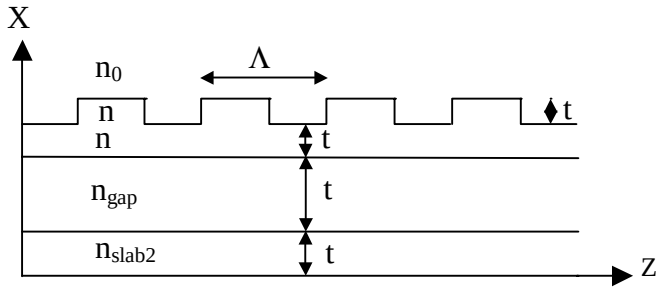

Fig. 1. Architectural scheme of one-stage GADC filter.

2. Design considerations

The conventional coupled-mode theory (CMT) [6] gives a well-known expression of the coupling coefficient k in the GADC filter, which can be written as:

$$k = \frac{\omega \varepsilon_o}{8} \int_{t_g} E_A^* \Delta n_g^2 E_B dx \tag{1}$$

where E_A, E_B are the normalized wavefunctions of the two compound modes of unperturbed structure (A even and B odd mode, respectively), Δn_g^2 is the relative permittivity change, as induced by the grating, and t_g is the grating thickness. Since the grating profile is a periodic index distribution along the GADC, its permittivity change depends on the coefficients of its own Fourier series expansion. In particular, in Eq. (1), only one coefficient is dominant, i.e.

#1787 - $15.00 US Received October 28, 2002; Revised November 11, 2002

the series expansion coefficient $n=1$ which minimizes the phase change between the two coupled waves. Therefore, the permittivity change for a rectangular profile becomes:

$$\Delta n_g^2 = \frac{(n_g^2 - n_o^2)}{\pi}\sin(\pi\frac{w}{\Lambda}) \tag{2}$$

where n_g, n_o are the grating and overlay refractive indices, respectively, Λ is the grating period, and w/Λ the duty cycle of the grating profile, being w the groove width. Therefore, the coupling strength can be appropriately modulated along the grating by changing its duty cycle.

In Fig. 2(a) the normalized coupling coefficient as a function of the grating duty cycle is shown for different profiles. The calculation has been carried out by using the coefficients of the Fourier series expansion of the relevant profile. The apodization functions used in this paper (and shown in Fig. 2) are in particular:

$Han(n) = 0.5[1-\cos(2\pi n/(N-1))]$ (Hanning)

$Ham(n) = 0.54 - 0.46\cos(2\pi n/(N-1))$ (Hamming)

$Blac(n) = 0.42 - 0.5\cos(2\pi n/(N-1)) + 0.08\cos(4\pi n/(N-1))$ (Blackman)

where n designates the generic grating period and N is the total number of periods (N odd).

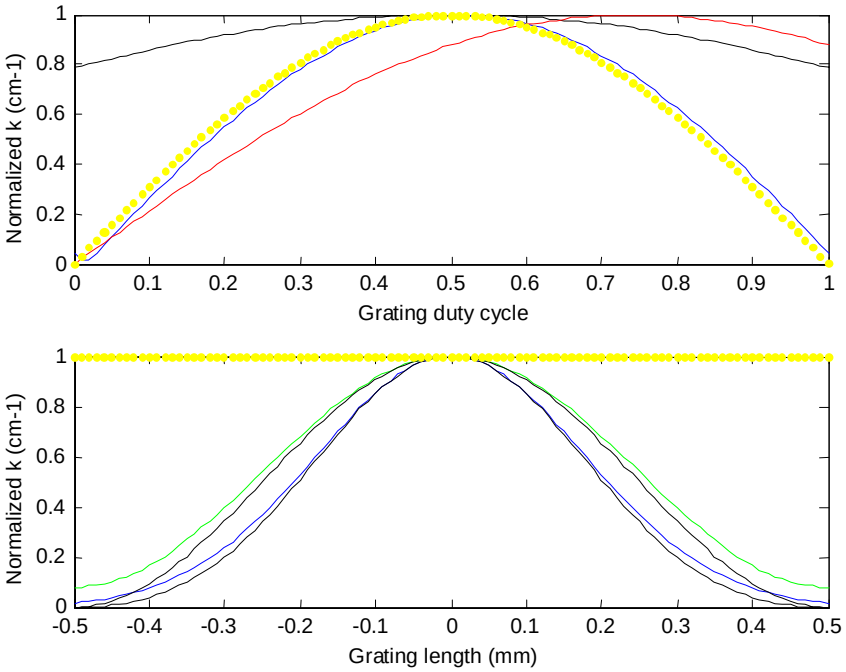

Fig. 2. (a) Normalized k (cm^{-1}) versus the grating duty cycle: rectangular (yellow); trapezoidal (blue); triangular (red); asymmetric triangular (black). (b) Normalized k versus the grating length (mm) for different apodization windows (yellow: uniform; blue: Hamming; black: Blackman; green: Gaussian; wider black line: Raised-cosine).

However, the CMT approach represents only a first-order approximation in the solution of GADC structures. The rigorous approach is based on the Floquet-Bloch formalism, where the influence of the grating over the characteristics of the leaky modes travelling in the coupler can be accurately taken into account, involving both space harmonics carrying power

#1787 - $15.00 US
Received October 28, 2002; Revised November 11, 2002

inside the grating and space harmonics carrying power outside the structure as radiating power. This approach, called leaky mode propagation (LMP), was firstly presented in [7] for the calculation of radiation losses in GADCs, then used in [8] for finding the resonance condition and, finally, applied in [9] for the optimal design of GADCs.

The LMP method allows a better understanding of the GADC operation principle and a more rigorous calculation of the coupling coefficient, in the form:

$$k = \frac{\omega \varepsilon_o}{8}\left(n_g^2 - n_o^2\right)\left[\int_{t_g} f_{-1}^{A^*} c_0 f_0^B dx + \int_{t_g} f_0^{A^*} c_0 f_{+1}^B dx + \int_{t_g} f_0^{A^*} c_1 f_0^B dx + \int_{t_g} f_{-1}^{A^*} c_1 f_{+1}^B dx\right] \qquad (3)$$

where A and B are the modes exchanging power inside the GADC, the mode A being composed by space harmonics (-1,0) with normalized field distributions (f_{-1}^A, f_0^A), and mode B by space harmonics (0,+1) with normalized field distributions (f_0^B, f_{+1}^B), respectively. In Eq. (3), c_0, c_1 designate the fundamental and first-order coefficient of the grating profile Fourier series expansion, respectively.

Therefore, Eq. (3) clearly shows that the accurate prediction of coupling coefficient allowed by LMP method is well different from that obtained by CMT in Eq. (1). In fact, the latter method cannot taken into account the influence of both the c_0, c_1 coefficients of the profile series expansion and the real field distributions in the device. For example, for rectangular profiles where $c_0 = w/\Lambda$ and $c_1 = (w/\Lambda)\ \sin c(w/\Lambda)$, it can be easily proved by using Eq. (3) that the coupling coefficient is proportional to the duty cycle even for $w/\Lambda \le 0.4$ [3], while the CMT approach gives a rather different estimation (see Eq. (2)). Therefore, very accurate predictions of k can be obtained by LMP rather than CMT approach for design purposes. The evaluation of accurate values of k means to strongly increase the filter fabrication precision in terms of the grating duty cycle apodization and, then, the filter performance in terms of bandwidth and SSR. The comparison of different grating profiles, made in Fig. 2(a), demonstrates that some shapes, i.e. rectangular or trapezoidal, allow to obtain the same coupling coefficient with two different values of duty cycles. There is no ambiguity in this circumstance, since only one value of duty cycle is practically chosen during the fabrication process, on the basis of the required fabrication tolerances. Moreover, Fig. 2(b) shows the coupling efficiency distribution along the GADC length, as apodized by a number of different functions. The apodization windows are always symmetric with respect to the centre of the GADC length.

The centre wavelength of the filter depends on the grating period calculated under the resonance condition [8-9]. This is a very critical aspect in the design of DWDM wavelength filters, since it strongly influences the selected centre wavelength. The CMT approach does not allow an accurate calculation of the period, i.e. the centre wavelength. In fact, the relative error can be larger than 0.7%, well different from the typical channel spacing in a 100 GHz DWDM system, about 0.05% (8 Å). Thus, the approximation of the period evaluation should result in a shift of the centre wavelength of more than 13 channels, which is unpractical for a "dense" system. This strong reduction of the number of system channels is also influenced by the GADC parameters (layer refractive indices and thicknesses, grating groove depth).

As the coupling coefficient, the resonance condition can be found with high accuracy by the LMP approach, the precision depending only on the number of space harmonics retained in the algorithm. Usually, a number of 23 space harmonics are enough to design the GADC filter with rectangular profile. As an example, we have calculated the resonance condition of the InGaAsP/InP structure presented in [10-11] (two stage filter as in Fig. 3), having refractive indices n_o =3.18, n_g = 3.482, n_{slab1} =3.482, n_{gap} =3.18, n_{slab2} =3.282, n_{sub} =3.18 and thicknesses

#1787 - $15.00 US Received October 28, 2002; Revised November 11, 2002

t_{slab1} =0.3 μm, t_{gap} =1.1 μm, t_{slab2} = 0.26 μm, t_g = 35 nm, at the wavelength of 1550 nm (see parameters in Fig. 1). The resonance occurs at $\Lambda = 16.8$ μm in case of squared profile ($w/\Lambda = 0.5$, TE polarization), instead of 18 μm as evaluated in [10] by CMT. This means a relative error greater than 7.1%, causing a filter centre wavelength shifting of more than 10 nm, that is larger than 12 filter channels in 100 GHz systems !. This example well shows how the CMT predictions are very poor when a highly selective filter is required.

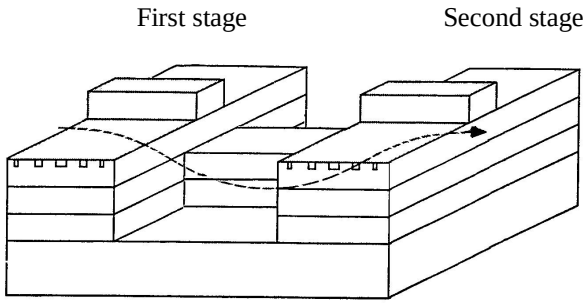

Fig. 3. Scheme of two stage grating-assisted filter.

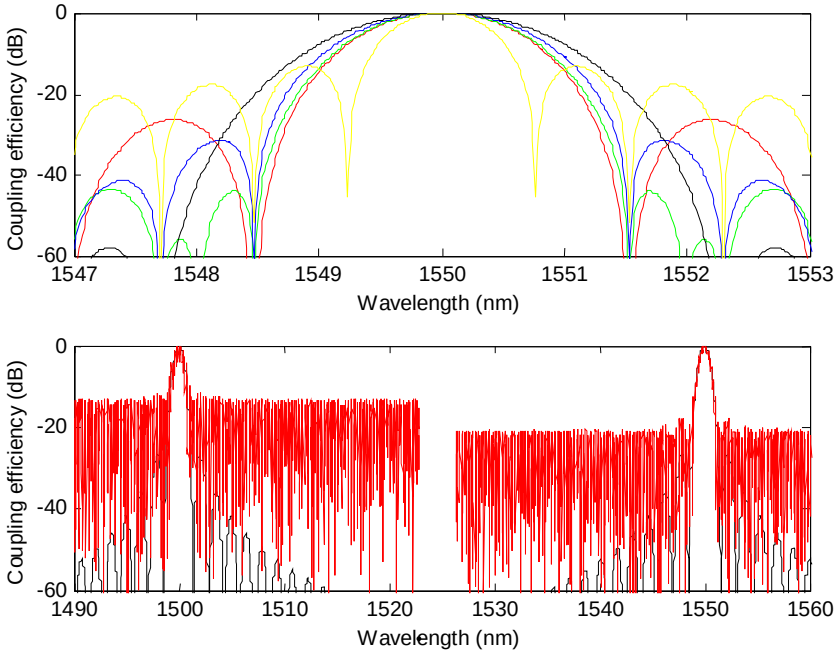

Fig. 4. (a) Coupling efficiency (dB) versus the wavelength (nm) for different filter apodizations: Tri=Triangular (red); Blac=Blackman (black); Rect= uniform (yellow); Hamming (green); Hanning (blue). (b) Coupling efficiency (dB) as a function of a tuned wavelength in case of triangular window by CMT (red line) and LMP (black line). GADC length is L = 1 mm.

#1787 - $15.00 US
Received October 28, 2002; Revised November 11, 2002

Moreover, the calculation of coupling coefficient by LMP gives $k = 26.5\,\mathrm{cm}^{-1}$, quite different from that obtained by CMT, i.e. $k = 19.3\,\mathrm{cm}^{-1}$. In Fig. 4(a) the wavelength spectra (dB) relevant to some apodization windows are sketched at the output of the one-stage filter. The best SSR is clearly obtained by the Blackman function, but at the expenses of a larger bandwidth. A narrower bandwidth can be obtained by triangular or Hamming functions. Table I summarizes the most significant parameters of various windows, together with the main requirements of DWDM systems (red section).

Table I. Characteristic parameters for various apodizations (L = 1 mm for each stage).

Apodization	*-3 dB bandwidth (nm)*		*Bandwidth (-20 dB)*	*SSR (dB)*
	One stage	Two stages		
Uniform	0.675	0.487	1.404	-13.26
Triangular	0.974	0.695	2.256	-26.52
Hamming	0.994	0.708	2.340	-44.03
Hanning	1.105	0.784	2.524	-31.46
Blackman	1.254	0.892	3.033	-58.11
DWDM systems: 100 GHz channel spacing	0.45		-	< -25
DWDM systems: 50 GHz channel spacing	0.25		-	< -30
DWDM systems: 25 GHz channel spacing	0.18		-	< -35

It is clear that the best performance in terms of SSR can be obtained by the Blackman function, while in terms of bandwidth by the uniform apodization. The bandwidth can be further linearly reduced by increasing the GADC length L of each stage. Therefore, the requirements of 100 GHz channel spacing DWDM systems could be for example satisfied by using two triangular windows each one at least 1.6 mm long. For more dense systems, having 25 GHz channel spacing (i.e. 250 channels 2Å spaced within a tunable range of 50 nm), only Hamming or Blackman windows could be used, at least 4 mm and 5 mm long for each stage, respectively. However, the apodization functions shown are more and more difficult to be fabricated. Good technological results in approximating the functions summarized in Table I could be obtained by using the state-of-the-art electron beam lithography, allowing an accuracy better than 0.1 μm in the definition of the grating groove width and period. We believe that the triangular apodization represents a very good trade-off among conflicting requirements, i.e. high SSR, narrow bandwidth and fabrication tolerances, for the fabrication of grating-assisted tunable filters for 100 GHz channel spacing DWDM systems. The design of these very sophisticated filters, having the critical parameters of Table I, is possible only by using the very accurate predictions of the rigorous LMP approach.

The tunability of GADC filters is obtained by applying a current (charge injection) to the upper slab waveguide, n_{slab1} (see Fig. 1). Depending on the injection, the refractive index of the semiconductor layer is decreased, changing the resonance condition (i.e. the centre wavelength which best matches the grating period). Figure 4(b) shows the shift of the channel wavelength by inducing a variation to the upper slab refraction index from 3.482 to 3.4 (tuning range of 50 nm). Further reductions of slab index can increase the tuning range. However, the tunability induces also a reduction of SSR, due to a reduction of coupling coefficient which depends on the term $n_g^2 - n_o^2$ (see Eq. 3). An asymmetry in the spectrum of coupling efficiency can be then observed in Fig. 4(b) for a triangular window. This asymmetry and its related spectral distortion is very significant when the filter is designed by the approximated CMT approach (red line). SSR values of –18 dB and –12 dB have been so

#1787 - $15.00 US Received October 28, 2002; Revised November 11, 2002

evaluated before and after the current injection. Much more accurate spectral responses can be obtained by designing by the LMP approach (black line). The asymmetry can be partially reduced or compensated by increasing the grating groove depth.

Finally, another important effect to be considered in the design of tunable GADC filters is the influence of the finite transverse dimensions of the GADC slabs. This has been evaluated as a first approximation by applying the effective index method to the transverse slab formed by three layers, i.e. $n_s = 3.18$, $n_{slab1} = 3.482$ and $n_s = 3.18$ (TM-polarized wave). The numerical results assert that if the upper slab has a transverse size $t_{trans,slab1} \geq 10$ μm, the TE-polarized wave field distribution and its effective index are not practically influenced by the waveguide sidewalls. In fact, in that case only the refractive index change "seen" along the GADC depth influences the field distribution of the two compound modes of the structure, coupled by the GADC grating. This result has been substantially confirmed by more accurate simulations performed by the beam propagation method [12]. In Fig. 5 the field distribution in the transverse section of the GADC filter (as in Fig. 3) is sketched, showing the negligible effect of the sidewalls along the horizontal direction.

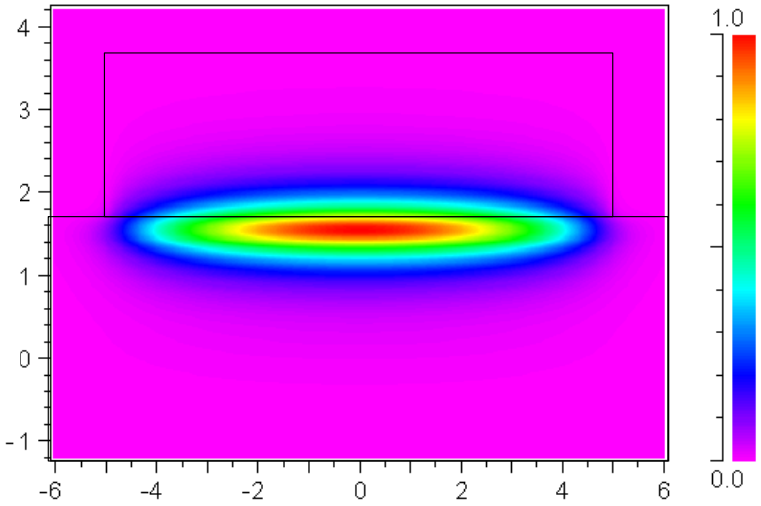

Fig. 5. Field distribution inside the GADC filter transverse section.

3. Conclusions

The most significant aspects in the design of tunable optical filters based on GADCs have been described and discussed using a sophisticated numerical technique based on the Floquet-Bloch formalism (LMP approach). Very accurate predictions of the GADC filter design parameters are so possible, including the resonance condition, the coupling coefficient and the apodization windows, to be used to satisfy the critical requirements of modern DWDM systems. The filter characteristics strongly depend on the technological parameters. SSRs larger than –58 dB, –3 dB bandwidths less than 1.8 Å, and tuning ranges wider than 50 nm can be obtained by designing by LMP two-stage GADC filters apodized by Blackman windows.

#1787 - $15.00 US
Received October 28, 2002; Revised November 11, 2002